Numerical investigation on broadband mid-infrared supercontinuum generation in chalcogenide suspended-core fibers*

Kundong Mo(莫坤东)[1], Bo Zhai(翟波)[1,†], Jianfeng Li(李剑峰)[1], E Coscelli[2], F Poli[2], A Cucinotta[2], S Selleri[2], Chen Wei(韦晨)[1], and Yong Liu(刘永)[1]

[1] *State Key Laboratory of Electronic Thin Films and Integrated Devices, School of Optoelectronic Information, University of Electronic Science and Technology of China, Chengdu* 610054, *China*
[2] *Information Engineering Department, University of Parma, Parma* 43124, *Italy*

(Received 5 July 2016; revised manuscript received 9 January 2017; published online 30 March 2017)

As_2S_3 and As_2Se_3 chalcogenide 3-bridges suspended-core fibers (SCFs) are designed with shifted zero-dispersion wavelengths (ZDWs) at around 1.5 μm, 2 μm, and 2.8 μm, respectively. A generalized nonlinear Schrödinger equation is used to numerically compare supercontinuum (SC) generation in these SCFs pumped at an anomalous dispersion region nearby their ZDWs. Evolutions of the long-wavelength edge (LWE), the power proportion in the long-wavelength region (PPL), and spectral flatness (SF) are calculated and analyzed. Meanwhile, the optimal pump parameters and fiber length are given with LWE, PPL, and SF taken into account. For As_2S_3 SCFs, SC from a 14 mm-long fiber with a ZDW of 2825 nm pumped at 2870 nm can achieve the longest LWE of ∼ 13 μm and PPL up to ∼72%. For As_2Se_3 SCFs, the LWE of 15.5 μm and the highest PPL of ∼ 87% can be achieved in a 10 mm-long fiber with ZDW of 1982 nm pumped at 2000 nm. Although the As_2Se_3 SCFs can achieve much longer LWE than the As_2S_3 SCFs, the core diameter of As_2Se_3 SCFs will be much smaller to obtain a similar ZDW, leading to lower damage threshold and output power. Finally, the optimal parameters for generating SC spanning over different mid-IR windows are given.

Keywords: supercontinuum generation, suspended-core chalcogenide fiber, nonlinear optics, fiber design

PACS: 42.81.–i, 42.81.Bm, 42.65.Sf, 42.81.Dp **DOI:** 10.1088/1674-1056/26/5/054216

1. Introduction

Mid-infrared broadband supercontinuum (SC) sources have been studied intensively in recent years because of their potential applications in many fields such as military,[1] gas detection,[2] spectroscopy,[3] and biomedical.[4] Mid-IR SC sources can be used in the so-called direct IR counter measures (DIRCM) because the response ranges of military detectors are 2.5–3.3 μm and 3.5–4.5 μm.[1] Mid-IR SC sources can also be used for gas detection since a lot of polluting gases and combustion products have strong absorption lines in the mid-IR region, i.e., NH_3 (2.1 μm), HF (2.5 μm), CH_4 (2.35 μm and 3.3 μm), HCHO (3.5 μm), HCl (3.5 μm), N_2O (3.9 μm and 4.5 μm), SO_2 (4 μm), CO_2 (4.25 μm), and CO (2.3 μm and 4.6 μm).[2] Mid-IR emitters offer rich possibilities for areas such as atmospheric pollution monitoring, industrial process control, leak detection, automotive engine exhaust analysis, non-invasive diagnostics, and ultrasensitive drug detection.[3] Mid-IR SC sources can also be applied into probing and controlling the ultrafast vibration of some important chemical bonds because many chemicals have their vibration or rotation spectra in this regime. In the biomedical field, many biological targets have their fundamental vibration absorption bands and lines in the mid-IR wavelength regime.[4] For example, the proteins show primary light absorption at 2.8–3.2 μm due to N–H and O–H bonds, while lipids exhibit absorptions in 3.2–3.6 μm associated with C–H stretching vibrations. Water is also one of these molecules that exhibit a set of strong absorption lines in the mid-IR region, especially near 3 μm and 6 μm, causing strong mid-IR absorption in human skin, which facilitates numerous biomedical applications in laser surgery, tissue ablation, and photo dermatology.

The first SC generation ranging from 400 nm to 700 nm was observed in bulk BK-7 glass with a pump source of 5 mJ picosecond pulses and 530 nm center wavelength.[5] Subsequently, the silica fibers began to be used for SC generation since they can provide enough length for nonlinear integration. Especially, the microstructure silica fibers which can be designed to provide strong nonlinearity and appropriate dispersion have been widely applied to generate SC. An SC generation in a microstructure silica fiber spanning from 0.4 μm to 2.4 μm has been demonstrated and a detailed numerical analysis of the SC generation in this fiber was given as well.[6] However, it is inadequate to choose the silica fiber for SC generation in the mid-IR regime due to its high transmission loss beyond 2.5 μm.[7] Some soft-glass fibers composed of chalcogenide, tellurite, or ZBLAN have a much broader IR trans-

*Project supported by the National Nature Science Foundation of China (Grant Nos. 61435003, 61377042, 61505024, and 61421002), Open Fund of State Key Laboratory of Advanced Optical Communication Systems and Networks, China (Grant No. 2015GZKF004), Open Found of Key Laboratory of Specialty Fiber Optics and Optical Access Networks, Shanghai University, China (Grant No. SKLSFO2014-07), and Open Fund of Science and Technology on Solid-State Laser Laboratory, China (Grant No. H04010501W2015000604).

†Corresponding author. E-mail: cqzhaibo@sina.com

© 2017 Chinese Physical Society and IOP Publishing Ltd

mission window, and thus are suitable for mid-IR SC generation. Owing to its high nonlinearity (nonlinearity is nearly 20 times that of silica),[8] tellurite glass has been extensively used to generate mid-IR SC. In order to achieve a broadband SC, the pump wavelengths generally should be close to the zero dispersion wavelengths (ZDWs) of the fiber.[6] Since the ZDW of the tellurite fiber is 2.24 μm,[9] the fiber needs to be designed as a microstructure or tapered fiber for shifting the ZDW to the shorter wavelength and implementing pumping in the anomalous dispersion regime close to the ZDW.[10–14] Although there have been several experimental and theoretical investigations reported about the mid-IR SC generation in the micro structured and tapered tellurite fibers, the longest wavelength edge cannot exceed 5 μm due to its relatively narrower infrared transparency window (0.4–5 μm).[10]

ZBLAN glass exhibits broad IR transparency with a 0.2–7 μm transmission window.[10] Simultaneously, the ZDW of a normal ZBLAN fiber is 1.62 μm,[15] and thus the pump sources at 1550 nm or 2000 nm can be employed to generate mid-IR SC in the normal or anomalous dispersion regime, respectively. However, the nonlinear refractive index n_2 of ZBLAN is only comparable to silica. Thus, a longer fiber length has to be used to provide enough nonlinearity.[8] A number of investigations on mid-IR SC generation in ZBLAN fiber pumping at around 1550 nm and 2000 nm have been reported.[16–24] Qin *et al.* demonstrated an SC from ultraviolet to 6.28 μm in a centimeter-long fluoride fiber pumped by a 1450 nm femtosecond laser.[19] Recently, the output power for SC generation in the ZBLAN fiber has been updated significantly. Yang *et al.* demonstrated an all fiber mid-IR SC from ∼ 1.9 μm to 4.3 μm with 13 W average output power in a single mode ZBLAN fiber pumped by the 2 μm MOPA system.[25] Using a similar system, Liu *et al.* increased the output average power of the SC to 21.8 W.[26] Jean *et al.* demonstrated an SC from 2.4 μm to 5.4 μm in a low-loss fluoroindate fiber pumped at 2.75 μm, with more than 82% of the total power beyond 3 μm.[27] However, the longest edge of SC in ZBLAN fiber is hard to exceed 7 μm due to the limitation of transparency and nonlinearity.

Chalcogenide glass, which is based on chalcogen elements S, Se, and Te, has the excellent IR transparency with broad IR transmission windows at 0.8–7 μm, 1–10 μm, and 2–12 μm, respectively.[28,29] It also exhibits very high nonlinearity, which approaches thousands of times that of silica.[30,31] Recently, the SC generation with the longest wavelength edge up to 13.3 μm has been demonstrated in a chalcogenide step-index fiber pumped by an optical parametric amplifier (OPA) at 6.3 μm.[32] Tonglei *et al.* experimentally demonstrated an SC generation spanning from 2 μm to 15.1 μm in a 3 cm-long chalcogenide step-index fiber with a 2.4 μm to 11 μm wavelength range tunable pump source.[33] However, for practical application, a pump source with shorter wavelength especially close to that which the fiber laser can achieve is favored, and thus the chalcogenide tapered or PCF should be used to shift the ZDW to the shorter wavelength. For the chalcogenide tapered fiber, an SC with bandwidth from 1.5 μm to 5 μm has been theoretically demonstrated in a tapered As_2S_3 fiber pumped at 2 μm with peak power of 1 kW.[34] Al-Kadry *et al.* have demonstrated an SC over two octaves from 1.1 μm to 4.4 μm in an As_2Se_3 micro-wires pumped by 1.94 μm pulses with low pulse energy of 500 pJ.[35] For chalcogenide PCF and MOF, Cheng *et al.* have demonstrated an SC spanning from 1.3 μm to 5.4 μm in a 2 cm-long $AsSe_2$–As_2S_5 hybrid MOF with ZDW of 3380 nm pumped by an OPO laser with center wavelength of ∼3389 nm and peak power of ∼ 1337 W.[36] A broad band mid-IR 0.9–9 μm SC has also been theoretically demonstrated in a concatenated fluoride and chalcogenide MOF with ZDW of 3550 nm pumped by a standard thulium laser with a pulse duration of 3.5 ps and peak power of 20 kW.[37] Wei *et al.* numerically investigated the high power mid-infrared SC generation in an As_2Se_3 PCF. The simulation results showed that the longest wavelength edge can attend 12 μm with 2.78 μm pump pulses.[38] Recently, Saini *et al.* theoretically demonstrated an SC spanning from 2 μm to 15 μm in a triangular-core graded-index PCF pumped by 4.1 μm pulses with 50 fs pulse duration and 3.5 kW peak power.[39]

Besides, suspended-core fibers (SCFs) are also an excellent candidate for further enhancing the nonlinear properties and for dispersion engineering. The small core and high NA of SCF ensure tight confinement of light and high nonlinearity. Besides, low loss, high air-filling fraction, and ultra-low mode field diameter have attracted designers to exploit SCFs for SC generation.[10,11] A mid-IR SC spanning from 1 μm to 4 μm has been experimentally shown in an As_2S_3 SCF with ZDW of 1660 nm pumped by an OPO laser with tunable wavelength from 1.7 μm to 2.6 μm,[10] while one spanning from 1.5 μm to 4.5 μm has also been achieved in a As_2S_3 SCF with ZDW of 2.52 μm pumped by an OPO laser with tunable wavelength from 2.2 μm to 2.6 μm.[11] Mouawad *et al.* have demonstrated a 0.6–4.1 μm SC in a 20 mm As_2S_3 SCF with ZDW of 3500 nm by pumping at 2.5 μm.[40] Very recently, Moller *et al.* demonstrated an SC spanning from 1.7 μm to 7.5 μm in an $As_{38}Se_{62}$ SCF with ZDW of 2400 nm pumped at 4.4 μm with pulse duration of 320 fs and peak power of 14.8 kW.[41] However, a comprehensive study devoted to a thorough analysis of the effects of all the pump and fiber parameters on the broadening, flatness, and power proportion of SC generation in chalcogenide SCFs has not been presented yet.

In this paper, we investigate and compare the SC generation in As_2S_3 and As_2Se_3 chalcogenide 3-bridges SCFs with different ZDWs. Variation of long wavelength edge, power

proportion in the long wavelength region, and spectral flatness (SF) with different pump parameters are also analyzed in detail. Finally, the optimal parameters for generating SC spanning over different mid-IR windows are given.

2. Numerical model for SC generation

To numerically study the SC generation in SCFs, pulses evolution inside the nonlinear fibers need to be described accurately. A better approach to include the frequency dependent nonlinear coefficient and the dispersion of the nonlinear response is to describe the generalized nonlinear Schrödinger equation (GNLSE) directly in the frequency domain as[42]

$$\frac{\partial \tilde{A}'(z,\omega)}{\partial z} = \mathrm{i}\bar{\gamma}(\omega)\exp(-\hat{L}(\omega)z) \times F\left\{\bar{A}(z,T)\int_{-\infty}^{\infty} R(T')\left|\bar{A}(z,T-T')\right|^2 \mathrm{d}T'\right\}, \quad (1)$$

with the frequency dependent nonlinear coefficient defined as

$$\bar{\gamma}(\omega) = \frac{n_2 n_0 \omega}{c n_{\mathrm{eff}}(\omega) A_{\mathrm{eff}}^{1/4}(\omega)}, \quad (2)$$

and

$$\bar{A}(z,T) = F^{-1}\left\{\frac{\tilde{A}(z,\omega)}{A_{\mathrm{eff}}^{1/4}(\omega)}\right\}, \quad (3)$$

$$\tilde{A}'(z,\omega) = \tilde{A}(z,\omega)\exp(-\hat{L}(\omega)z), \quad (4)$$

where $\tilde{A}(z,\omega)$ is the complex spectral envelope as a function of the distance along the fiber, and implementing $T = t - \beta_1 z$ to transform into a co-moving frame at the envelope group velocity β_1^{-1}. $\hat{L}(\omega)$ is the linear operator given by

$$\hat{L}(\omega) = \mathrm{i}[\beta(\omega) - \beta(\omega_0) - \beta_1(\omega_0)(\omega-\omega_0)] - \alpha(\omega)/2, \quad (5)$$

which models linear propagation effects, with α being the power attenuation and β_k being the dispersion coefficients associated with the Taylor series expansion of the propagation constant $\beta(\omega)$ about ω_0. $R(t)$ is the Raman response function including both the Kerr (instantaneous) contribution and the Raman (delayed) contribution, which is given by

$$R(t) = (1-f_{\mathrm{R}})\delta(t-t_{\mathrm{e}}) + f_{\mathrm{R}}h_{\mathrm{R}}(t) = (1-f_{\mathrm{R}})\delta(t-t_{\mathrm{e}}) + f_{\mathrm{R}}\frac{\tau_1^2+\tau_2^2}{\tau_1\tau_2^2}\exp\left(-\frac{t}{\tau_2}\right)\sin\left(\frac{t}{\tau_1}\right)\Theta(t), \quad (6)$$

where f_{R} is the fractional contribution of the delayed Raman response. Raman delayed function $h_{\mathrm{R}}(t)$ could be described by τ_1 and τ_2. $\Theta(t)$ is the Heaviside step function and $\delta(t)$ is the Dirac delta function.

$n_{\mathrm{eff}}(\omega)$ is the frequency dependent effective index of the guided mode. n_0 is the linear refractive index when determining nonlinear refractive index n_2. The frequency dependence of the nonlinear coefficient $\bar{\gamma}(\omega)$ in Eq. (2), arising through the frequency variation of A_{eff} and n_{eff}, is explicitly evident. Although it cannot be directly compared with the standard nonlinear coefficient $\gamma = n_2\omega_0/(cA_{\mathrm{eff}})$,[43] γ at the center wavelength will be repeatedly mentioned below to describe the nonlinearity. Another advantage of this formulation of GNLSE is that equation (1) could be seen as an ordinary differential equation. This means that it can be integrated directly using the Runge–Kutta technique because the stiff dispersive part has been removed though the change of variables given in Eq. (4).[44] Notice that a border-absorbing time window condition is adopted in the numerical simulation to avoid fast components returning and colliding with the main pulse.[6]

3. Design of highly nonlinear suspended core fibers for SC generation

Figure 1(a) shows the cross-section of the highly nonlinear SCF considered in the present analysis. It is characterized by three large air-holes in the cladding, separated by the same number of thin glass bridges with thickness t, which create the core at their intersection. The core diameter d_{c} is defined as the diameter of the largest circumference which can be inscribed into the core. In order to design technologically-feasible chalcogenide fibers or, at least, structures that can be obtained by tapering over lengths of several centimeters,[45,46] values of d_{c} in the range between 1 μm and 5 μm and of t between 0.15 μm and 0.45 μm are considered for the preliminary

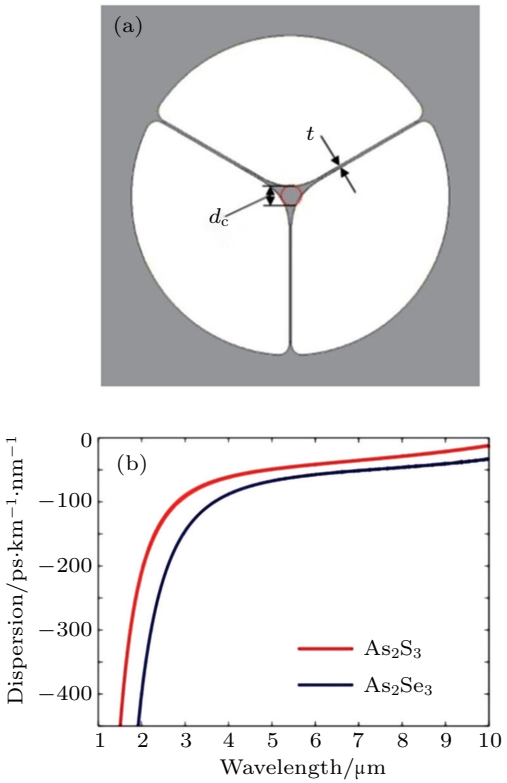


Fig. 1. (color online) (a) Cross-section of the chalcogenide SCF. (b) Dispersion parameter versus wavelength of the two chalcogenide glasses As_2S_3 and As_2Se_3.

simulations. The length of the struts is fixed to 20 μm in order to prevent leakage of the fundamental mode into the cladding. Finally, two chalcogenide glasses, As_2S_3 and As_2Se_3, providing good properties in terms of IR transparency, nonlinearity, and drawing capability, but different contributions in terms of material dispersion, are chosen for the design of SCFs suitable for mid-IR SC generation. Notice that the refractive index n of the chalcogenide glasses is calculated according to the Sellmeier equation

$$n^2(\lambda) = 1 + \sum_i \frac{A_i \lambda^2}{\lambda^2 - \lambda_i^2}, \tag{7}$$

where proper values of the coefficients A_i and λ_i are used for As_2S_3 and As_2Se_3.[47] A full-vector modal solver based on the finite-element method[48] is applied to calculate the SCF fundamental mode in the wavelength range of interest.

Dispersion engineering guidelines obtained with a previous analysis on the dispersion properties of As_2S_3 SCFs with three, five, and six bridges[49] are exploited to design nonlinear chalcogenide fibers suitable for SC generation in the mid-IR. In particular, the core diameter and the bridge thickness of SCFs made of both As_2S_3 and As_2Se_3, are properly chosen to obtain a ZDW around the wavelengths of 1.5 μm, 2 μm, and 2.8 μm, which can be considered for efficiently pumping the SC generation. As shown in Fig. 1(b), which reports the dispersion curves of the two glasses in the wavelength range between 1 μm and 10 μm, the ZDW of As_2Se_3 is longer than that of As_2S_3, which is around 4.9 μm. As a consequence, it is necessary to significantly blue-shift the As_2Se_3 ZDW towards the desired wavelength range by introducing a strong waveguide dispersion component through the SCF design, which is obtained, according to previous results, with a reduced core diameter. Figures 2(a) and 2(b) show the dispersion curves in the wavelength range between 1 μm and 3.5 μm of the SCFs made of As_2S_3 and As_2Se_3, respectively, which have ZDWs around 1.5 μm, 2 μm, and 2.8 μm. The main characteristics of the proposed fibers are summarized in Table 1. It is important to underline that, as expected, the As_2Se_3 fiber providing a ZDW suitable for a given pumping wavelength has a smaller core than the one of the corresponding SCF made of As_2S_3 glass. Moreover, larger core fibers provide a longer ZDW, regardless of the chalcogenide glass chosen. It is interesting to underline that the As_2S_3 SCF with the smallest core, that is d_c = 1 μm, has two ZDWs in the considered wavelength range. In particular, the first one is around 1530 nm, and the second one around 3030 nm. Notice that it is impossible to design an SCF made of As_2Se_3 with ZDW around 1550 nm also satisfying the requirement imposed by the fiber technological feasibility of a core diameter larger than 1 μm. The normalized frequency V for an SCF can be calculated by $V_{\text{eff}} = a_{\text{eff}}(n_{\text{co}}^2 - n_{\text{FSM}}^2)^{1/2} 2\pi/\lambda$.[6]

According to the single-mode condition of $V_{\text{eff}} < 2.405$, the cut-off wavelengths of these designed SCFs are shorter than 1.5 μm. Thus, the effects of high order modes on the SC generation can be ignored. The effective mode area is defined as

$$A_{\text{eff}}(\omega) = \frac{\left(\int\int_{-\infty}^{+\infty} |F(x,y,\omega)|^2 \mathrm{d}x\mathrm{d}y\right)^2}{\int\int_{-\infty}^{+\infty} |F(x,y,\omega)|^4 \mathrm{d}x\mathrm{d}y}, \tag{8}$$

where F is the transverse modal distribution. Modeling based on the finite element method predicts the transverse modal distribution.[48]

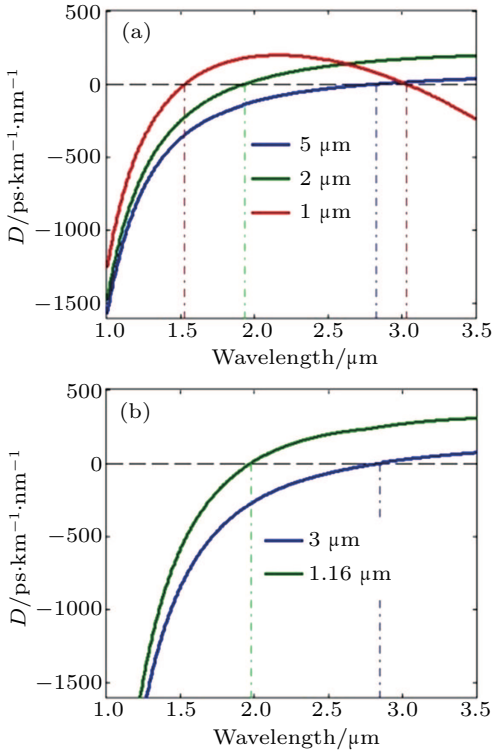


Fig. 2. (color online) Disperse curves of proposed (a) As_2S_3-based and (b) As_2Se_3-based chalcogenide SCFs.

Figure 3(a) shows the spectral dependence of the material propagation loss of As_2S_3 and As_2Se_3 chalcogenide glasses in the long-wavelength range.[50] The confinement loss should be taken into account when generating SC spectra in small core fibers. We simulate the confinement loss of the proposed SCFs and those of 1–2 μm diameter SCFs are shown in Fig. 3(b), the confinement loss of 3 μm and 5 μm diameter SCFs is ignored because it is less than 0.5 dB/cm even at 15 μm.

Table 1. Main characteristics of the 3-bridges SCFs.

SCF material	d_c/μm	t/μm	ZDW/nm	A_{eff}/μm^2
As_2S_3	1	0.35	1530/3030	0.95@1550 nm
As_2S_3	2	0.35	1935	2.84@2000 nm
As_2S_3	5	0.7	2825	15.56@2890 nm
As_2Se_3	1.16	0.35	1982	1.24@2000 nm
As_2Se_3	3	0.35	2855	6.01@2890 nm

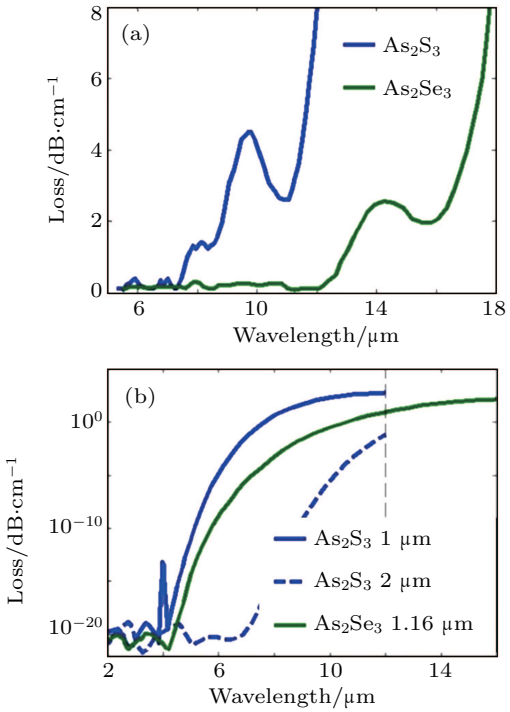


Fig. 3. (color online) (a) Material propagation loss of As_2S_3 and As_2Se_3 chalcogenide glasses in the long-wavelength range and (b) the confinement loss of 1–2 μm diameter As_2S_3 SCFs.

4. Results and discussion

In the last section, As_2S_3-based and As_2Se_3-based SCFs are designed to obtain ZDWs below 3 μm. In this section, SC generation in these SCFs pumped around ZDWs are simulated and analyzed.

4.1. Mid-IR SC generation in As_2S_3-based SCF

In our simulation, the f_R, τ_1, and τ_2 of As_2S_3-based SCFs are 0.031, 15.2 fs, and 230.5 fs,[51] respectively. The maximum pump peak power for SC generation is estimated according to the optical damage of materials. When the pulse duration is shorter than 1000 fs, the maximum energy fluence at the facet of the chalcogenide waveguide should not exceed 0.05 J/cm^2.[52] For an input pulse duration range from 200 fs to 1000 fs, the peak power damage threshold is estimated to be ~1000 W/μm^2. The effective mode areas of the three As_2S_3-based SCFs with ZDWs of 1530/3030 nm (two ZDWs), 1935 nm, and 2825 nm are ~ 0.95 μm^2, ~ 2.84 μm^2, and ~ 15.56 μm^2, respectively. Thus, the maximum pump peak powers are estimated to be ~ 950 W, ~ 2840 W, and ~ 15560 W, respectively.

Here, we compare the SC spectra generated in the three proposed fibers pumped at an anomalous GVD regime nearby ZDW. Because the ZDWs of the three SCFs are 1530/3030 nm, 1935 nm, and 2825 nm, we choose the ultra-short pump sources centered at 1550 nm, 2000 nm, and 2870 nm respectively. The pump peak power is set to be the estimated maximum values. The input pulse duration is fixed at 800 fs. Figure 4 shows the SC spectral and temporal pulse evolutions in As_2S_3-based SCFs with ZDWs of 1530/3030 nm, 1935 nm, and 2825 nm. As shown in Fig. 4(c), the SC output from a 20 mm As_2S_3 SCF with ZDW of 2825 nm pumped by input pulses with a center wavelength of 2870 nm and a peak power of 15560 W has the longest long-wavelength edge (LWE) (40 dB down from the peak of the spectrum) up to ~ 12 μm among the three SCFs. The output SCs from the SCFs with ZDWs of 1530/3030 nm and 1935 nm are broadened to ~ 4.5 μm and ~ 8 μm, respectively, as shown in Figs. 4(a) and 4(b). Generally, SC generation with anomalous GVD regime pumping is dominated by soliton-related effects. In the initial stage of SC generation, SC broadening mainly depends on the SPM-induced approximately symmetrical spectrum. After the relative narrow broadening, for input pulses duration exceeding 200 fs, the dramatic broadening of the spectrum appears with the soliton fission, whereby a higher-order soliton perturbed by Raman scattering breaks up into a series of lower-amplitude subpulses.[6] In this stage of SC generation, the temporal pulses break up and the generation of distinct spectral peaks in the anomalous GVD regime can be clearly identified due to the soliton fission and the Raman self-frequency shift of the ejected constituent fundamental solitons, as shown in Figs. 4(g)–4(i). Because the effective mode area is ~ 15.56 μm^2 and the nonlinear coefficient γ is ~ 0.5908 W^{-1}·m^{-1} at 2870 nm. The soliton fission length L_{fiss} is estimated to be ~ 10.5 mm according to $L_{\text{fiss}} \sim L_D/N$,[6] where the dispersion length $L_D = 1.02$ m, the nonlinear length $L_{NL} = 1/\gamma P_0 = 0.109$ mm, and the soliton number $N = \sqrt{L_D/L_{NL}} = 97$. As shown in Fig. 4(i), the temporal pulses break up at ~ 11 mm of the fiber, which is in coincidence with the calculated L_{fiss}. The soliton number N in the fiber with ZDW of 2825 nm is 97, which is larger than that of 86 in the fiber with ZDW of 1935 nm. The larger N means that it could break up to more fundamental solitons. Thus, more red-shift frequency components appear induced by the Raman self-frequency shift effect. The high nonlinearity of As_2S_3 allows a very low peak power threshold for SC generation in fiber, the soliton number N of 5–8 can be obtained with a lower peak power less than 10 W at ~ 2870 nm, which is beneficial for stimulating soliton-related effects in the long wavelength range. Meanwhile, the ultra-short fiber length brings relative low propagation loss even beyond the wavelength of 12 μm. Thus, such a high pump peak power of 15560 W is enough for stimulating SC generation in the long wavelength range. We should note that the fiber with a core diameter of 1 μm has two ZDWs of 1530 nm and 3030 nm, proving an anomalous GVD regime of 1530–3030 nm, which means that the soliton-related effects only appear in a relatively narrow wavelength range. Although the soliton number N of the input pulse with a duration of 800 fs and a peak power

of 950 W in this fiber is calculated to be the largest value of ~ 132 among the three fibers as a result of its huge nonlinear coefficient γ of ~ 18.044 $W^{-1}\cdot m^{-1}$ at 1550 nm, the narrow anomalous GVD regime limits the continuous broadening to a longer wavelength. As shown in Fig. 4(a), the output SC from a 20 mm long fiber has a flat spectrum in 1–3.8 μm. Thus, the SCF with a ZDW of 2825 nm is an ideal candidate for achieving a comparatively broader spectrum with higher output power, while the fiber with two ZDWs of 1530/3030 nm is conducive to generating a flat spectrum.

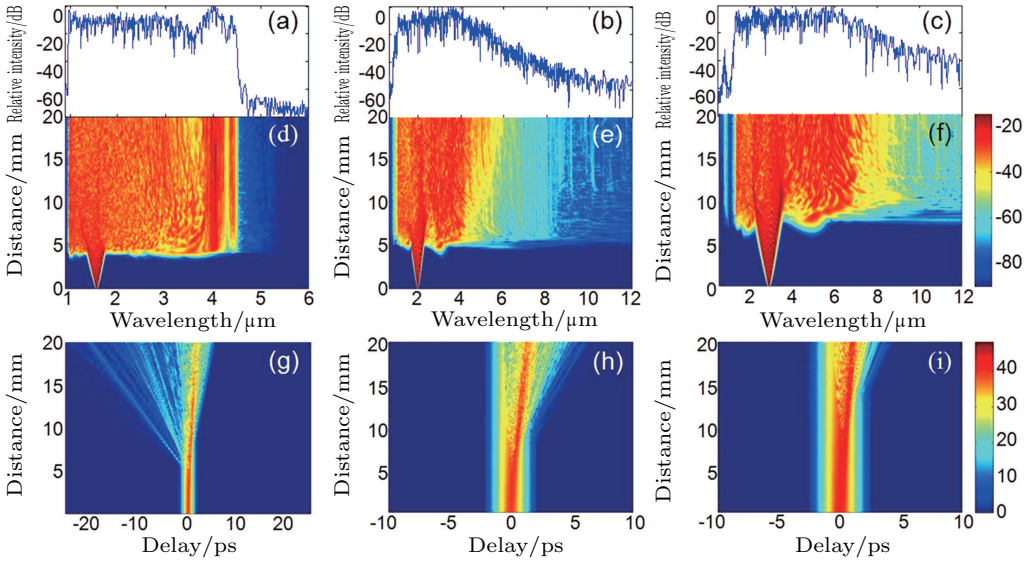


Fig. 4. (color online) (a)–(c) Output SC, (d)–(f) spectral evolution, and (g)–(i) temporal evolution in the three proposed As_2S_3-based SCFs. (a), (d), (g) SC generation in SCF with two ZDWs of 1530/3030 nm pumped by input pulses with pulse duration of 800 fs, peak power of 950 W, and center wavelength of 1550 nm. (b), (e), (h) SC generation in SCF with a ZDW of 1935 nm pumped by input pulses with pulse duration of 800 fs, peak power of 2840 W, and center wavelength of 2000 nm. (c), (f), (i) SC generation in SCF with a ZDW of 2825 nm pumped by input pulses with pulse duration of 800 fs, peak power of 15560 W, and center wavelength of 2870 nm.

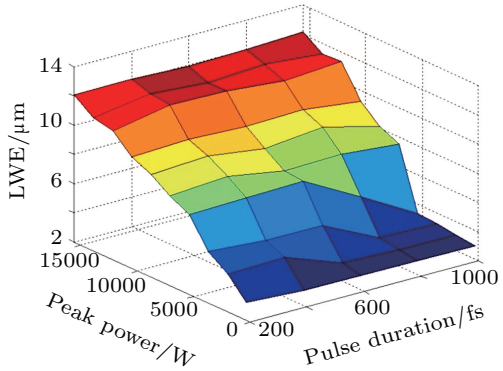


Fig. 5. (color online) LWE (40 dB down from the peak of spectrum) changed with the pulse duration and peak power for the 20 mm As_2S_3 SCF with a ZDW of 2825 nm, the center wavelength of the input pulses is 2870 nm.

To obtain the broadest SC spectrum generated in the As_2S_3-based SCF with a ZDW of 2825 nm pumped by an input pulse of 2870 nm, we must choose an input pulse with optimal duration and peak power. Figure 5 shows the LWE (40 dB down from the peak of the spectrum) changed with different input pulse durations and peak powers, the fiber length is fixed at 20 mm. With the increasing peak power, the LWE increases until ~ 12 μm. The LWE changes slightly with the increasing pulse duration especially in the high peak power region. To study the influence of the pulse duration on broadening, the SC spectral and temporal evolutions along this 20 mm SCF pumped by 200 fs and 1000 fs input pulses are compared in Fig. 6. The key difference of evolutions between these two cases lies in the initial spectral broadening stage. Because the same peak power of 15560 W is used in these two cases, the soliton fission length L_{fiss} increases from ~ 4 mm to ~ 12 mm as the pulse duration increases from 200 fs to 1000 fs. It corresponds with the temporal pulse evolution as shown in Figs. 6(e) and 6(f). Obviously, with a shorter pumping optical pulse duration, the appearance of dramatic broadening induced by soliton-related effects requires a shorter propagation distance. However, the change of the pulse duration only leads to a small change in the SC width that outputs from the 20 mm-long fiber.

To further understand the influence of the input pulse duration, the evolution of LWE and PPL along the 20 mm As_2S_3-based SCFs with d_c of 5 μm and ZDW of 2825 nm pumped by optical pulses with different pulse durations are simulated, where the input pulse peak power is 15560 W, and the durations are 200 fs and 1000 fs, as shown in Fig. 7(a) and 7(b), respectively. With the pulse duration of 200 fs, the LWE and PPL increase dramatically at the beginning 5 mm, and then the PPL beyond 3 μm increases slightly until it reaches $\sim 80\%$, while the LWE declines slightly with increasing distance. The longest LWE of ~ 12.5 μm is achieved at the distance of ~ 10 mm. In the 1000 fs duration case, the LWE and PPL in-

crease dramatically at the beginning 10 mm, and then the PPL beyond 3 μm increases until it reaches ∼ 75%, while the LWE decreases from its peak value of ∼ 13 μm at the fiber length of ∼ 14 mm to 12.3 μm at 20 mm. The slight decline of LWE from its peak results from the larger propagation loss in the long-wavelength region and less red-shift component. To simply describe the spectral flatness with the 20 dB bandwidth, the standard deviation (SD) of spectral density with 20 dB bandwidth is calculated as shown in Figs. 7(c) and 7(d). In order to focus on the differences of SF between different cases, the spectrum density data for SD are smoothed using a moving average filter. The definition for the standard deviation S of the spectrum density sample data x_i is

$$S = \left[\frac{1}{n}\sum_{i=1}^{n}(x_i - \bar{x})^2\right]^{1/2}, \quad \bar{x} = \frac{1}{n}\sum_{i=1}^{n} x_i, \tag{9}$$

where x_i is the spectrum density sample value at each wavelength with 20 dB bandwidth, n is the sample number, and $\bar{x}$ is the average of those sample values. Here, the smaller the SD of spectral density means the flatter the spectrum. It is

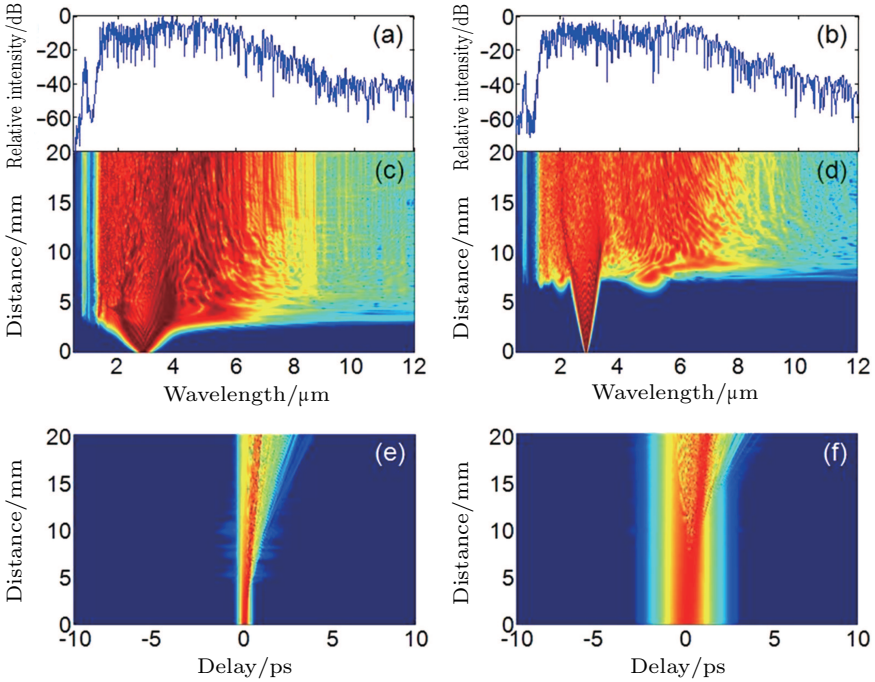


Fig. 6. (color online) (a), (b) Output SC, (c), (d) spectral evolution, and (e), (f) temporal evolution in As_2S_3 SCFs with a ZDW of 2825 nm. (a), (c), (e) Pumped by input pulses with pulse duration of 200 fs, peak power of 15560 W, and center wavelength of 2870 nm. (b), (d), (f) Pumped by input pulses with pulse duration of 1000 fs, peak power of 15560 W, and center wavelength of 2870 nm.

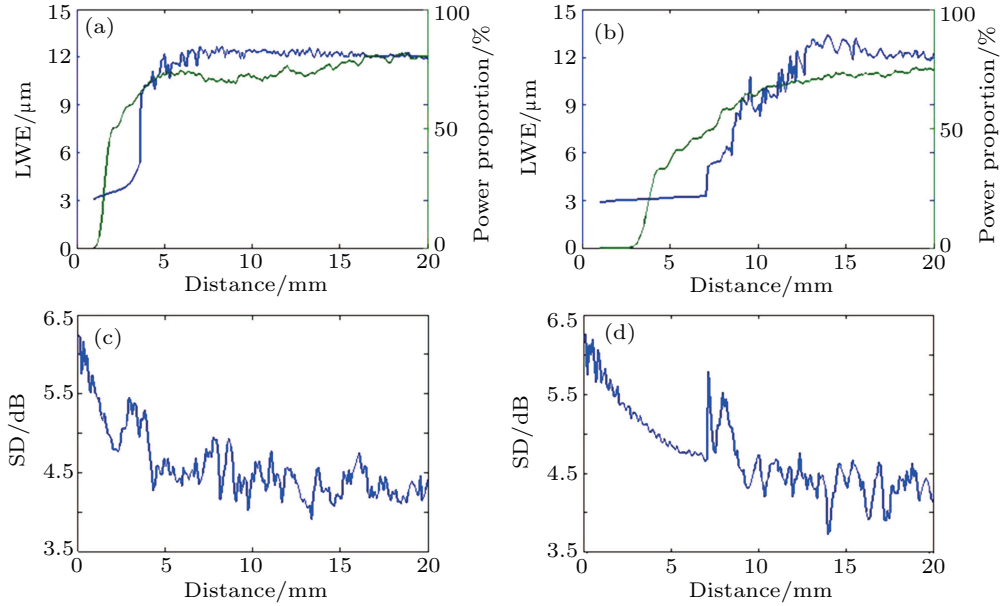


Fig. 7. (color online) Pumped by input pulses with pulse durations of (a), (c) 200 fs and (b), (d) 1000 fs, peak power of 15560 W, and center wavelength of 2870 nm. The blue and green curves in panels (a) and (b) show the LWE and the PPL beyond 3 μm, respectively. (c), (d) The SD of spectrum density with 20 dB bandwidth versus propagation distance in the As_2S_3 SCF with a ZDW of 2825 nm.

observed that the variations of SD on propagation distance for both cases are similar. With the pulse duration of 200 fs, the SD decreases in the first 2 mm, and then rises in 2–3 mm resulting from the appearance of some new frequency components with soliton fission. Then, it continues to decrease because of the generation of more new frequency components making the spectrum flatter. Finally, the SD of the spectrum just vibrates near 4.5 dB after $\sim$ 5 mm propagation, which means that the SF of SC changes slightly after $\sim$ 5 mm propagation. Pumped by 1000 fs pulses, the distance for spectrum broadening is around 7 mm, which is longer than $\sim$ 2 mm in the 200 fs case. In conclusion, comparing the 200 fs pulse duration case with the 1000 fs case in the As_2S_3-based SCF with a ZDW of 2825 nm, the 200 fs case can obtain SC with a higher PPL of $\sim$ 80% but the 1000 fs case can obtain a longer LWE of $\sim$ 13 μm. Moreover, to achieve the SC with the highest LWE and comparatively low SD of the spectrum, the 1000 fs case needs a longer fiber than the 200 fs case.

4.2. Mid-IR SC generation in As_2Se_3-based SCF

The SC generation in the designed As_2Se_3-based chalcogenide SCFs will be discussed in this section. The f_R, τ_1, and τ_2 of the As_2Se_3-based SCFs are 0.148, 23 fs, and 164.5 fs,[53] respectively. We assume that the peak power damage threshold of the As_2Se_3-based SCFs is close to the damage threshold of the As_2S_3-based SCFs. Since the effective mode areas of the two As_2Se_3-based SCFs with ZDWs of 1982 nm and 2855 nm are $\sim 1.24\ \mu m^2$ and $\sim 6.01\ \mu m^2$, the maximum pump peak powers are estimated to be $\sim$ 1240 W and $\sim$ 6010 W, respectively.

Firstly, we compare the SC generation in the proposed two fibers pumped at an anomalous GVD regime nearby ZDWs. The pump peak powers are set to be the maximum value estimated before and the input pulse duration is fixed to 800 fs. Figure 8 shows the SC spectral evolution in the two SCFs with sufficient length for complete broadening. Since the ZDWs of these two proposed SCFs are 1982 nm and 2855 nm, we choose the ultrashort pump sources with wavelengths of 2000 nm and 2870 nm to pump them, respectively. As shown in Fig. 8(a), the SC generation in the 10 mm SCF with a ZDW of 1982 nm pumped by the pulse with a wavelength of 2000 nm and peak power of 1240 W has a longer LWE to $\sim$ 15 μm than the SC generated in the 20 mm SCF with a ZDW of 2855 nm. The longer LWE for the As_2Se_3 SCF with d_c of 1.16 μm results from the stronger soliton-related propagation effects such as soliton fission and soliton self-frequency shift. For the 1.16 μm SCF, the nonlinear coefficient γ is 38.188 $W^{-1}\cdot m^{-1}$ at 2000 nm, which is much larger than that of 5.466 $W^{-1}\cdot m^{-1}$ at 2870 nm for the SCF with d_c of 3 μm. The corresponding soliton numbers N are 220 and 183 under their maximum pump peak power, respectively. Meanwhile, the higher nonlinearity of the smaller core SCF allows a lower soliton fission threshold of 0.4 W at $\sim$ 2000 nm for SC generation.

The As_2Se_3-based SCF with a ZDW of 1982 nm is more suitable for generating a broader SC spectrum. To obtain the broadest SC spectrum pumped by the input pulse of 2000 nm, we must choose the optimal input pulse duration and peak power.

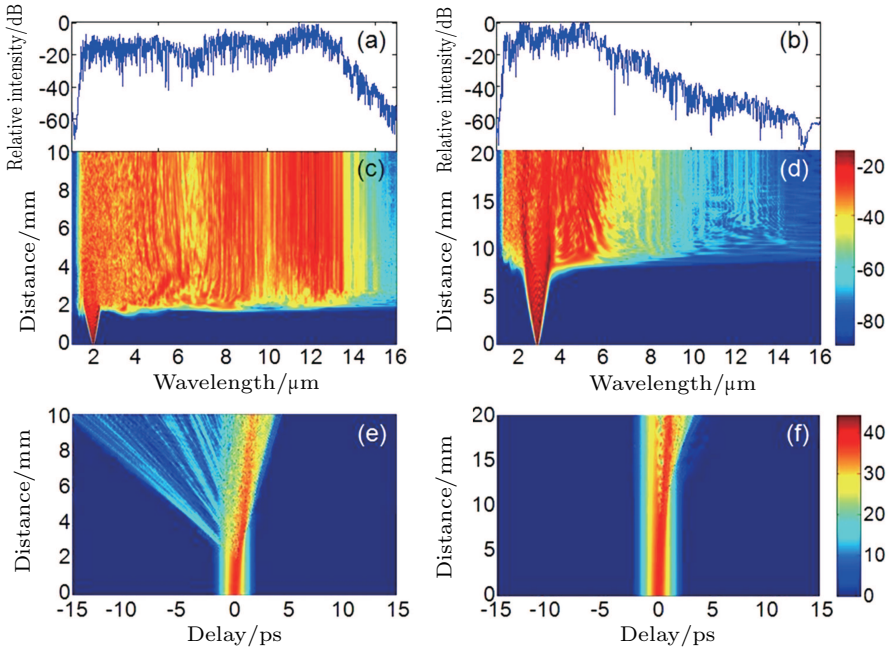


Fig. 8. (color online) (a), (b) Output SC, (c), (d) spectral evolution, and (e), (f) temporal evolution in the two proposed As_2Se_3-based SCFs. (a), (c), (e) SC generation in SCF with a ZDW of 1982 nm pumped by input pulses with pulse duration of 800 fs, peak power of 1240 W, and center wavelength of 2000 nm. (b), (d), (f) SC generation in SCF with a ZDW of 2855 nm pumped by input pulse with pulse duration of 800 fs, peak power of 6010 W, and center wavelength of 2870 nm.

Figure 9 shows the LWE (40 dB down from the spectrum peak) changed with different input pulse durations and peak powers, where the fiber length is fixed to 10 mm firstly; a discussion about the choice of fiber length will be given later. The LWE increases smoothly and slightly with the increasing pulse peak power and duration at the relatively high peak power region. So the input pulse with a pulse duration of 1000 fs and a peak power of 1240 W is the proper choice.

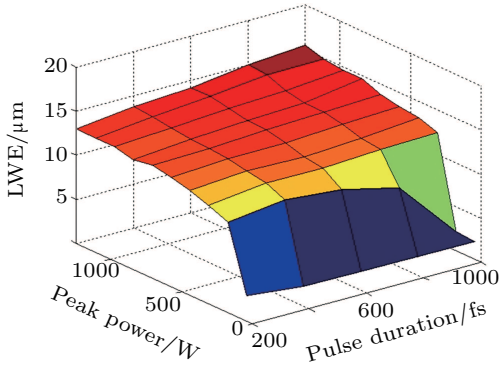


Fig. 9. (color online) LWE changed with the pulse duration and peak power for the 10 mm As_2Se_3 SCF with a ZDW of 1982 nm, the center wavelength of the input pulse is 2000 nm.

The evolutions of LWE and PPL along the 10 mm As_2Se_3-based SCFs with d_c of 1.16 μm pumped by pulses with different pulse durations are simulated, where the input pulse peak power is 1240 W and duration is 200 fs and 1000 fs, as shown in Figs. 10(a) and 10(b), respectively. It is observed that the two cases have a similar length of ∼ 3 mm for the SC completely broadening. Figure 10(a) shows that the LWE increases dramatically in the distance of 1–2 mm, then it is essentially unchanged at ∼ 13 μm with increasing distance. The PPL beyond 3 μm increases up to ∼ 78% after a sharp growth in the first 4 mm. In Fig. 10(b), the LWE increases dramatically up to 16 μm from 2 mm to 3 mm, and then, it decreases slightly to ∼ 15.5 μm at 10 mm with the increasing distance. The PPL beyond 3 μm increases up to ∼ 87% after a sharp growth in the beginning 4 mm. Obviously, the SC generated using longer pulses can obtain longer LWE and higher PPL beyond 3 μm, which results from more Raman red-shift frequency components associated with larger soliton number N. Longer input pulses induce higher soliton order N and larger input pulse energy. On one hand, higher soliton order N is beneficial to the new spectrum components generated with soliton self-frequency shift. On the other hand, with larger input pulse energy, there will be more energy in the long wavelength range, which leads to a larger overall spectral width at the fiber output within the scope of fs input pulses. After determining the peak power and duration, the optimal fiber length could be discussed. The SD of spectral density with 20 dB bandwidth for SC with pump pulse of 1000 fs is calculated as shown in Fig. 10(d). It changes slightly in the distance beyond 4 mm after a dramatic decline, which means that the SF of SC changes slightly after 4 mm propagating in fiber. In conclusion, with an input pulse duration of 1000 fs and a peak power of 1240 W, the SC generated in a ∼ 10 mm As_2Se_3-based SCF with a ZDW of 1982 μm could obtain a long LWE of 15.5 μm, the highest PPL beyond 3 μm, and comparatively high SF.

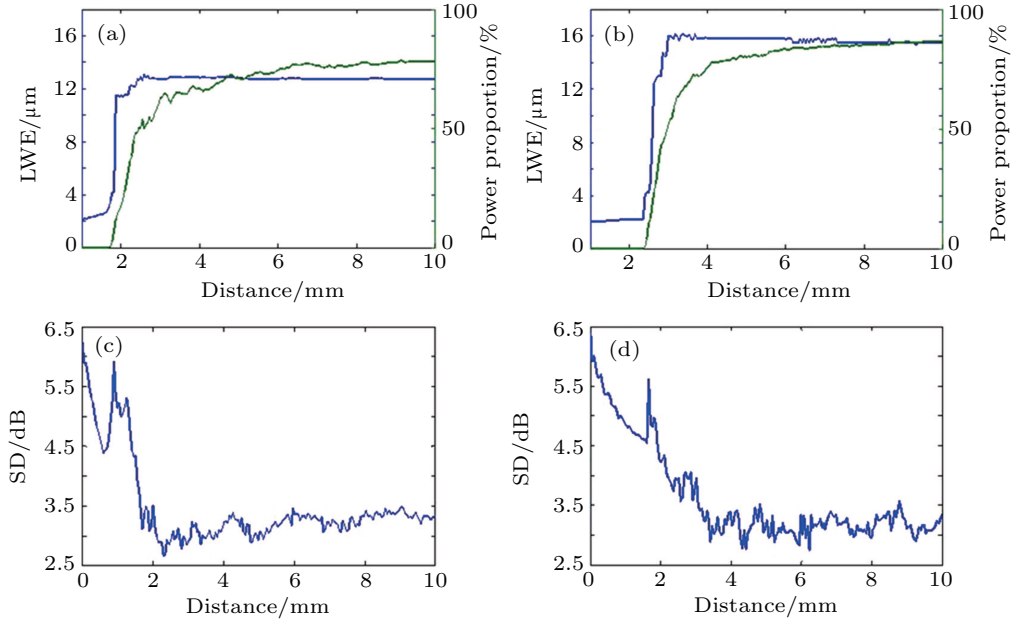


Fig. 10. (color online) Pumped by input pulses with pulse duration of (a), (c) 200 fs and (b), (d) 1000 fs, peak power of 1240 W, and center wavelength of 2000 nm. The blue and green curves in panels (a) and (b) show the LWE and the PPL beyond 3 μm, respectively. (c), (d) The SD of spectrum density with 20 dB bandwidth versus propagation distance in the As_2Se_3 SCF with a ZDW of 1982 nm.

4.3. Generating SC spanning over different mid-IR windows

Compared with As_2S_3-based chalcogenide SCFs, As_2Se_3-based chalcogenide SCFs could obtain a broader SC since they have a higher nonlinear refractive index n_2 of 1.5×10^{-17} $W^{-1}\cdot m^{-1}$ and a wider spectral transmission window. With the same ZDWs, the core diameter of As_2Se_3 SCF is smaller, which could obtain an ultrahigh nonlinear coefficient so that an ultra-short fiber length less than 10 mm is enough for the complete broadening of SC. In addition, such a short fiber length brings low total propagation loss even the attenuation coefficient is large. The low peak power threshold for high-order nonlinear effects resulted from the ultrahigh nonlinear coefficient also makes the LWE broaden further. However, smaller core diameters lead to lower damage threshold, which limits the output average power. To obtain similar ZDWs, the As_2Se_3 SCFs need a smaller core diameter than the As_2S_3 SCFs. For example, with ZDW nearby 2870 nm, the core diameter of As_2S_3 SCF is 5 μm, but for As_2Se_3 SCF it is 3 μm which is more difficult to fabricate. Table 2 lists the optimal pump source and fiber parameters for SC generated in As_2S_3 and As_2Se_3 SCFs and the corresponding power proportion and spectral SD in the mid-IR windows of 3–5 μm, 3–8 μm, and 3–12 μm. The chosen pump source pulse durations range from 200 fs to 1000 fs, and the maximum pump peak power is determined by the fiber damage threshold related to diameter d_c of SCFs. To obtain the 3–5 μm SC, the As_2S_3 SCF with ZDW of 2825 nm is the best choice among the three proposed As_2S_3 SCFs, and the As_2Se_3 SCF with ZDW of 2855 nm is an appropriate choice among the designed two As_2Se_3 SCFs. Compared with the As_2S_3 SCF, the As_2Se_3 SCF obtains higher 3–5 μm power proportion and lower 3–5 μm spectral SD of SC so that the As_2Se_3 SCF with ZDW of 2855 nm is the better candidate for 3–5 μm SC generation. To obtain the 3–8 μm SC, obviously the As_2S_3 SCF with ZDW of 2825 nm is the better candidate since it can obtain larger 3–8 μm power proportion while the 3–8 μm spectral SD is similar to As_2Se_3 SCF's. For the 3–12 μm SC, the As_2Se_3 SCF with ZDW of 1982 nm is an ideal candidate since it can obtain smaller 3–12 μm spectral SD with power proportion in 3–12 μm close to that of As_2Se_3 SCF.

Table 2. Optimal pump source and chalcogenide SCF parameters for generating SC spanning over different mid-IR windows.

Wavelength range/μm	SCF material	Fiber ZDW/nm	Fiber length/mm	Pulse wavelength/nm	Pulse peak power/W	Pulse duration/fs	Power proportion	Spectral SD/dB
3–5	As_2S_3	2825	~ 10	2870	15560	200	56%	4.2
3–5	As_2Se_3	2855	~ 10	2870	6010	500	57%	3.8
3–8	As_2S_3	2825	~ 14	2870	15560	1000	69%	5.5
3–8	As_2Se_3	1982	~ 8	2000	1240	200	43%	5.1
3–12	As_2S_3	2825	~ 14	2870	15560	1000	70%	9.8
3–12	As_2Se_3	1982	~ 10	2000	1240	1000	67%	4.8

5. Conclusion

We optimize the input pulse parameters and fiber length for generating the broadest SC in As_2S_3-based and As_2Se_3-based chalcogenide SCFs with different ZDWs and core diameters. For SC generation in As_2S_3-based SCFs, among the three proposed SCFs, the SCF with a core diameter of 5 μm and a ZDW of 2825 nm generates the broadest spectrum with LWE of ~13 μm pumped by input pulse with a center wavelength of 2870 nm and a peak power of 15560 W. In addition, compared with longer pulse duration pumping, shorter pulse duration pumping needs shorter fiber and would obtain SC with shorter LWE but higher PPL in the As_2S_3 SCF with a ZDW of 2825 nm. For SC generation in As_2Se_3-based SCFs, among the proposed two SCFs, the 1.16 μm diameter SCF with a ZDW of 1982 nm generates the broadest spectrum with LWE up to ~15.5 μm after propagating ~ 10 mm pumped by input pulse with a center wavelength of 2000 nm, a pulse duration of 1000 fs, and a peak power of 1240 W.

References

[1] Bekman H H P T, Heuvel J C, Putten F J M and Schleijpen R 2004 *Proc. SPIE* **56** 27

[2] Mukherjee A, der Porten S V and Patel C K N 2010 *Appl. Opt.* **49** 2072

[3] Thorpe M J, Hudson D D, Moll K D, Lasri J and Ye J 2007 *Opt. Lett.* **32** 307

[4] Paluszkiewicz C, Kwiatek W M, Banas A, Kisiel A, Marcelli A and Piccinini A 2007 *Vib. Spectrosc.* **43** 237

[5] Alfano R R and Shapiro S L 1970 *Phys. Rev. Lett.* **24** 584

[6] Dudley J M, Gentry G and Coen S 2006 *Rev. Mod. Phys.* **78** 1135

[7] Izawa T, Shibata N and Takeda A 1977 *Appl. Phys. Lett.* **31** 33

[8] Vogel EM, Weber M J and Krol D M 1991 *Phys. Chem. Glasses* **32** 231

[9] Fujino S and Morinaga K 1997 *J. Non-Cryst. Solids* **222** 316

[10] Savelii I, Mouawad O, Fatome J, Kibler B, Désévédavy F, Gadret G, Jules J C, Bony P Y, Kawashima H, Gao W, Kohoutek T, Suzuki T, Ohishi Y and Smektala F 2012 *Opt. Express* **20** 27083

[11] Domachuk P, Wolchover N A, Cronin-Golomb M, Wang A, George A K, Cordeiro C M B, Knight J C and Omenetto F G 2008 *Opt. Express* **16** 7161

[12] Liao M, Chaudhari C, Qin G, Yan X, Suzuki T and Ohishi Y 2009 *Opt. Express* **17** 12174

[13] Qin G, Yan X, Kito C, Liao M, Suzuki T, Mori A and Ohishi Y 2010 *J. Appl. Phys.* **107** 043108

[14] Qin G, Yan X, Liao M, Mori A, Suzuki T and Ohishi Y 2011 *Laser Phys.* **21** 1115

[15] France P W, Carter S F, Moore M W and Day C R 1987 *Brit. Telecommun. Technol. J.* **5** 28

[16] Hagen C L, Walewski J W and Sanders S T 2006 *IEEE Photon. Technol. Lett.* **18** 91

[17] Xia C, Kumar M, Cheng M, Hegde RS, Islam M N, Galvanauskas A, Winful H G and Terry F L 2007 *Opt. Express* **15** 865

[18] Qin G, Yan X, Kito C, Liao M, Chaudhari C, Suzuki T and Ohishi Y 2009 *Opt. Lett.* **34** 2015

[19] Qin G, Yan X, Kito C, Liao M, Chaudhari C, Suzuki T and Ohishi Y 2009 *App. Phys. Lett.* **95** 1611031

[20] Kulkarni O P, Alexander V V, Kumar M, Freeman M J, Islam M N, Terry F L, Neelakandan M and Chan A 2011 *J. Opt. Soc. Am. B* **28** 2486

[21] Agger C, Petersen C, Dupont S, Steffensen H, Lyngsø J K, Thomsen C L, Thøgersen J, Keiding S R and Bang O 2012 *J. Opt. Soc. Am. B* **29** 635

[22] Eckerle M, Kieleck C, Świderski J, Jackson S D, Mazé G and Eichhorn M 2012 *Opt. Lett.* **37** 512

[23] Heidt A M, Price J H V, Baskiotis C, Feehan J S, Li Z, Alam S U and Richardson D J 2013 *Opt. Express* **21** 24281

[24] Xia C, Xu Z, Islam M N, Terry F L, Freeman M J, Zakel A and Mauricio J 2009 *IEEE J. Sel. Top. Quantum Electron* **15** 422

[25] Yang W, Zhang B, Xue G, Yin K and Hou J 2014 *Opt. Lett.* **39** 1849

[26] Liu K, Liu J, Shi H-X, Tan F-Z, and Wang P 2014 *Opt. Express* **22** 24384

[27] Jean-Christophe G, Vincent F, Jean-yves C, Samuel P, Marcel P, Real V and Martin B 2016 *Opt. Lett.* **41** 1756

[28] Churbanov M F 1992 *J. Non-Cryst. Solids* **140** 324

[29] Sanghera J S, Nguyen V Q, Pureza P C, Kung F H, Miklos R and Aggarwal I D 1994 *J. Lightwave Tech.* **12** 737

[30] Lenz G, Zimmermann J, Katsufuji T, Lines M E, Hwang H Y, Spälter S, Slusher R E, Cheong S W, Sanghera J S and Aggarwal I D 2000 *Opt. Lett.* **25** 254

[31] Harbold J M, Ilday F Ö and Wise F W 2002 *Opt. Lett.* **27** 119

[32] Petersen C R, Moller U, Kubat I, Zhou B B, Dupont S, Ramsay J, Benson T, Sujecki S, Abdel-Moneim N and Tang Z Q 2014 *Nat. Photon.* **8** 830

[33] Cheng T, Nagasaka K, Tuan T H, Xue X, Atsumoto M M, Tezuka H, Suzuki T and Ohishi Y 2016 *Opt. Lett.* **41** 2117

[34] Hu J, Menyuk C R, Shaw L B, Sanghera J S and Aggarwal I D 2013 *Opt. Commun.* **293** 116

[35] Al-Kadry A, Amraoui M El, Messaddeq Y and Rochette M 2014 *Opt. Express* **22** 31131

[36] Cheng T, Kanou Y, Xue X, Deng D, Matsumoto M, Misumi T, Suzuki T and Ohishi Y 2014 *Opt. Express* **22** 23019

[37] Kubat I, Petersen C R, Moller U V, Seddon A, Benson T, Brilland L, Mechin D, Moselund P M and Bang O 2014 *Opt. Express* **22** 3959

[38] Wei C, Zhu X, Norwood R A, Song F and Peyghambarian N 2013 *Opt. Express* **21** 29488

[39] Saini T S, Kumar A and Sinha R K 2015 *J. Lightwave Tech.* **33** 3914

[40] Mouawad O, Picot-Clemente J, Amrani F, Strutynski C, Fatome J, Kibler B, Desevedavy F, Gadret G, Jules J C, Deng D, OhishiY and Smektala F 2014 *Opt. Lett.* **39** 2684

[41] Moller U, Yu Y, Kubat I, Petersen C R, Gai X, Brilland L, Mechin D, Caillaud C, Troles J, Luther-Davies Band Bang O 2015 *Opt. Express* **23** 3282

[42] Laegsgaard J 2007 *Opt. Express* **15** 16110

[43] Kibler J M D B and Coen S 2005 *Appl. Phys. B* **81** 337

[44] Hult J 2007 *J. Lightwave Tech.* **25** 3770

[45] El-Amraoui M, Fatome J, Jules J C, Kibler B, Gadret G, Fortier C, Smektala F, Skripatchev I, Polacchini C F, Messaddeq Y, Troles J, Brilland L, Szpulak M and Renversez G 2010 *Opt. Express* **18** 4547

[46] Gao W, Liao M, Yan X, Kito C, Kohoutek T, Suzuki T, El-Amraoui M, Jules J, Gadret G, Désévédavy F, Smektala F and Ohishi Y 2011 *Appl. Phys. Express* **4** 102601

[47] Klocek P 1991 *Handbook of Infrared Optical Materials* (Marcel: Dekker)

[48] Poli F, Cucinotta A and Selleri S 2007 *Photonic Crystal Fibers Properties and Applications* (Dordrecht: Springer Series in Material Science)

[49] Coscelli E, Poli F, Li J, Cucinotta A and Selleri S 2015 *IEEE Photonics Journal* **7** 1

[50] Shiryaev V S and Churbanow M F 2013 *J. Non-Cryst. Solids* **377** 225

[51] Gao W, El-Amraoui M, Liao M, Kawashima H, Duan Z, Deng D, Cheng T, Suzuki T, Messaddeq Y and Ohishi Y 2013 *Opt. Express* **21** 9573

[52] Yu Y, Gai X, Wang T, Ma P, Wang R, Yang Z, Choi D Y, Madden S and Luther-Davies B 2013 *Optical Materials Express* **3** 1075

[53] Salem A B, Cherif R, Zghal M and Electromagnet A 2011 *Raman Response of a Highly Nonlinear As_2Se_3-based Chalcogenide Photonic Crystal Fiber* (Marrakesh: Piers 2011 Progress in Electromagnetics Research Symposium) p. 1256